HAL
open science

Photosystem-II shutdown evolved with Nitrogen fixation in the unicellular diazotroph Crocosphaera watsonii

Sophie Rabouille, Pascal Claquin

▶ To cite this version:

Photosystem-II shutdown evolved with Nitrogen fixation in the unicellular diazotroph *Crocosphaera watsonii*

Sophie Rabouille[1,2*] and Pascal Claquin[3,4]

5   **Running title**: PSII shutdown in *C. watsonii*

Abstract

Protection of nitrogenase from oxygen in unicellular cyanobacteria is obtained by temporal separation of photosynthesis and diazotrophy, through transcriptional and

10   translational regulations of nitrogenase. But diazotrophs can face environmental situations in which N_2 fixation occurs significantly in the light, and we believe that another control operates to make it possible. The nighttime shutdown of PSII activity is a peculiar behavior that discriminates *C. watsonii* WH8501 from any other phototroph, whether prokaryote or eukaryote. This phenomenon is not only due to the

15   plastoquinone pool redox status and suggests that the sentinel D1 protein, expressed in periods of nitrogen fixation, is inactive. Results demonstrate a tight constraint of oxygen evolution in *C. watsonii* as additional protection of nitrogenase activity and suggest a possible recycling of cellular components.

Keywords

[1] Sorbonne Universités, UPMC Univ Paris 06, UMR 7093, LOV, Observatoire océanologique, F-06230, Villefranche/mer, France.
[2] CNRS, UMR 7093, LOV, Observatoire océanologique, F-06230, Villefranche/mer, France
[*] To whom correspondence should be addressed. Email: srabouille@obs-vlfr.fr; phone: +33(0)493 763 832. Address: Laboratoire d'Océanographie de Villefranche (LOV), UMR 7093, Station Zoologique, F-06230, Villefranche/mer, France
[3] Université de Caen-Normandie, BOREA, Caen, France
[4] CNRS-7208, IRD-207, MNHN, UPMC, UniCaen, BOREA, Caen, France

20   unicellular cyanobacteria/ light regime/ diazotroph/ electron transport/ continuous cultures/ *Crocosphaera*

Abbreviations: Chl*a*: chlorophyll *a*; ETR: electron transport rate; LD: Light:Dark; LHC: light harvesting complex; PAM: pulse amplitude modulated; PSII: photosystem II; rETR: relative ETR; UCYN: unicellular diazotrophic cyanobacteria

25

Introduction

First isolated and described by Waterbury and Rippka (1989), *Crocosphaera watsonii* WH8501 was more recently classified within group B, unicellular diazotrophic cyanobacteria (UCYN) and unveiled as a new substantial player in the marine

30   nitrogen cycle (Zehr et al., 2001; Falcon et al., 2002; Montoya et al., 2004; Zehr, 2011). Nitrogen fixation in diazotrophic cyanobacteria is tightly regulated, both at the transcriptional (Huang et al., 1988; Colon-Lopez et al., 1997; Toepel et al., 2008; Pennebaker et al., 2010; Shi et al., 2010) and physiological (Dron et al., 2012; Dron et al., 2013) levels, in response to environmental constraints. In particular, the

35   nitrogenase enzyme is extremely sensitive to oxygen (Staal et al., 2007; Compaore and Stal, 2010) leading cells to develop strategies to protect the nitrogenase from the denaturing effects of oxygen. The filamentous *Trichodesmium* spp show unique abilities to both temporally and spatially separate nitrogen fixation from photosynthesis (Berman-Frank et al., 2001) while in photo-autotrophic UCYN in

40   which there is no direct connection between cells, only a temporal decoupling can occur (Fay, 1992; Gallon, 1992). The nitrogenase enzyme is also further protected from oxygen by enhanced respiration rates (Fay, 1992; Gallon, 1992; Großkopf and LaRoche, 2012). Nitrogen fixation is thus observed in the dark in cultivated UCYN

grown under a 12:12 Light:Dark (LD) regime (e.g. Mitsui et al., 1986; Waterbury et
al., 1988; Mohr et al., 2010). But in nature, phytoplankton experiences a highly
dynamic light environment. First, light and dark periods are often unbalanced in
regions where these organisms naturally occur. Then, mixing in the surface layer also
leads to fluctuating LD regimes that largely deviate from the regular, square or even
sinusoidal regimes usually applied in the laboratory. Hence, although activities of
photosynthesis and nitrogen fixation are kept apart by diel,
transcriptional/translational regulations, light:dark and dark:light transitions still
represent a risk for them to occur at the same time. We therefore question how UCYN
maintain truly separated activities of photosynthesis and nitrogen fixation when the
time period theoretically devoted to the latter (i.e. the dark phase) is getting shorter.
Previous studies performed on *C. watsonii* showed a decrease in both the
photosynthetic capacity (Großkopf and LaRoche, 2012) and the maximal photosystem
II (PSII) quantum yield (F_v/F_m) during the dark period (Wilson et al., 2010). Wilson *et
al*. (2010) proposed that this decrease was mainly due to the reduction of the PQ pool,
which plays a central role in photosynthesis, respiratory and nitrogen fixation
metabolisms, but they did not consider any regulation on the PSII complex itself.

We investigated how capacities of photosynthesis and nitrogen fixation partition
around the LD cycle, observing the effect of three bell-shaped, light:dark (LD)
regimes on continuous cultures of *Crocosphaera watsonii*, with 8, 12 and 16 hours
light per 24h (8L:16D, 12L:12D and 16L:8D, respectively). We pictured the diel
patterns of PSII photosynthetic capacities through a close monitoring of the quantum
yield of PSII, which informs on the oxidation state of the plastoquinone pool and
therefore, on electron transfer rate from PSII (Kromkamp and Forster, 2003). We
describe a very unique photosynthetic dynamics in the dark and close to light

transitions, unreported in any phototroph so far. We believe that a tight regulation

70 blocks PSII operation to insure complete protection of the nitrogenase from oxygen

evolution. The mechanisms responsible for such regulation are discussed.

Results

The peculiar photosynthetic dynamics of *C. watsonii*

75 We measured photosynthetic parameters on continuous cultures exposed to three LD

regimes. Culture replicates showed strong and consistent repeatability, with similar

dynamics. The maximum, relative electron transport rate ($rETR_{opt}$) of PSII retrieved

from all photosynthesis-light response curves (PI curves; Fig. 1) was plotted against

time on Figure 2a (16L:8D), 1b (12L:12D) and 1c (8L:16D). The observed changes

80 denote important variations in PSII capacity during the day. All culture treatments

demonstrate a marked build up of PSII activity during the first half of the light period,

peaking around the mid light phase, followed by a decrease in the second half of the

light period. Fitted values of $rETR_{opt}$, α and I_{opt}, obtained from the four-day

measurements also present the same, consistent and typical diel dynamics (Fig. 3).

85 Figures 2 and 3 seem to further indicate that, for all three parameters ($rETR_{opt}$, α and

I_{opt}), the peak actually occurs after about 8 hours of light. This apparent periodicity is

observed independently of the three imposed illumination regimes (16L:8D, 12L:12D

and 8L:12D), and sustains in time as cultures are maintained at equilibrium.

During the light phase, cells undergo state transitions when recording light-response

90 curves. Exposure to the dark first triggered a transition to state II, which progressively

reverted to state I as cells experienced the first light steps, as revealed by the increase

in the maximum fluorescence ($F_m < F_m'$, Fig. 4a). Most striking is the null variable

fluorescence (both measured and fitted) during the dark period, whatever the light regime, leading to null rETR values (Fig. 1 & 2). A consistent, absence of activity was observed around PSII at night under all light regimes. In cells sampled in the dark phase, the maximum fluorescence equaled the transient fluorescence at all steps ($F_m = F_0$ and $F_m' = F_t'$, Fig. 4c). Because variable fluorescence did not recover during the light-response curves, F_v/F_m were null, and so were the F_v'/F_m' obtained under all tested actinic lights. Application of light pulses showed no effect on the maximum fluorescence, pointing to (i) an inactivated state of PSII and (ii) the absence of state transition. In the very early light phase, the response was similar to that observed in the dark, with a null or extremely low variable fluorescence (again, $F_m = F_0$ and $F_m' = F_t'$, Fig. 4b). Under the 12L:12D regime, no PSII activity was detected at both light transitions (light onset and dark onset): variable fluorescence decreased to zero values before the onset of the dark, and remained null in the early light phase. A different behavior appeared in the other two treatments: cultures exposed to a 16L:8D regime showed a measurable, although low, variable fluorescence at the dark-to-light transition only, while those exposed to 8L:16D showed a low, residual activity at the light-to-dark transition only.

110

Discussion

On the replicability of culture experiments

In the present work, the three sets of experiments were carried out using duplicate cultures. The experimental results obtained in all treatments show very good reproducibility between the two duplicates, both in terms of dynamics and amplitude

of the observed processes, asserting the validity of the observed physiological responses. Culture density was low enough to ensure homogeneous light distribution within the vessels and no shaded area, which simplifies the analysis of photosynthetic

120 efficiency as compared to reactors with strong light gradients (Zarmi et al., 2013). However, some difference in amplitude between the duplicate cultures appears in the 8L:16D experiment: the measured $rETR_{opt}$ is higher in culture 1 than in culture 2, suggesting that one replicate was photosynthetically more efficient than the other. Yet, both still follow the same daily dynamics; this discrepancy probably denotes a

125 slight difference in the energetic status of cells and thus does not affect the conclusions discussed in the following as for the diel regulation of processes. One might wonder on the cause of such difference, though. Considering that a slight difference in carbon content per cell was also reported by Dron and colleagues (2013) in the same culture treatment, we speculate that a difference in air bubbling in the

130 culture might have caused a lower CO_2 availability in culture 2, leading to a lower photosynthetic efficiency and lower carbon storage. This difference in culture treatments did not affect the processes dynamics discussed both in the work of Dron and colleagues (2013); but they would become critical if mass budgets were to be derived. These observations highlight how critical it is to finely control environmental

135 conditions applied to cultures in order to avoid experimental biases.

Nitrogen fixation in UCYN: how to tread on middle ground

Daily biomass acquisition in UCYN-B such as *C. watsonii* is related to their ability to tread on middle ground: that is, handle N_2 fixation in an oxygen evolving, phototrophic cell, although nitrogenase is irreversibly deactivated by oxygen. In the

140 present work, we bring evidence for an actual down-regulation of PSII photosynthetic efficiency when nitrogen fixation is needed in the early or late light phase.

Phycobilisomes movement optimizes photosynthetic efficiency in the light

Efficiency of photosynthesis first relies on the conversion of photonic energy into chemical energy, which is accurately pictured by a monitoring of the fluorescence yield of PSII, F_v/F_m. When acquiring a PI curve, the fluorescence response obtained at each light step allowed to estimate photosynthetic parameters like the photosynthetic activity rETR(I), the optimal photosynthetic capacity and the efficiency ($rETR_{opt}$, α) (Krause and Weis, 1984). The cellular chlorophyll content or the number of light harvesting complexes (LHC, in eukaryotes) or phycobilisomes (in red algae and in most cyanobacteria) associated to PSII and PSI can, for instance, modulate the photosynthetic status of cells. Fluctuations in $rETR_{opt}$ (Fig. 2) picture the diel changes in PSII potential activity, the i.e. the maximal electron transport measured that cells could yield if stimulated with an optimal irradiance. The present rETR data brought two important information on the growth dynamics of *Crocosphaera*. First, the fact that $rETR_{opt}$, α and I_{opt} all seem to peak after about eight hours of light hints towards the presence of an active internal clock, which the light regimes applied in this study did not alter or change. Second, the synchronicity between $rETR_{opt}$ and the irradiance peak in all cultures indicates that highest photosynthetic activity is observed when irradiance is also highest (Fig. 3). At any time, estimated values of I_{opt} were always higher than the applied irradiance in the cultures (Fig. 3) pointing to an absence of photoinhibition in all cultures and a photoacclimated state of cells, which show optimized photosynthetic response and high photoacclimation capacities. The photosynthetic apparatus is ready, should more light energy be available, in particular in cultures exposed to the shorter light phase, as suggested by the highest observed I_{opt} values.

A photosynthetic machinery short-circuited in the dark

Fluorescence kinetics in *C. watsonii* systematically reveals a decrease in electron transport towards the end of the light period, as well as an absence of fluorescence variation in the dark. Dark initiation triggers a transition of cells to state II. Also, respiration of carbohydrate reserves is expected to increase upon dark onset, and drive a transition to the low fluorescent state (state II) (Mullineaux and Allen, 1986). But even if in state II with all phycobilisomes attached to PSI, cells should initiate a transition back to state I upon illumination by the actinic light during the PI records. We also performed such measurements during the dark phase, applying a saturation pulse to DCMU treated samples in order to force a transition back to state I (Campbell et al., 1998). When using DCMU, fluorescence is expected to rise to the level of Fm, without possible decrease. But fluorescence did not increase upon application of light in untreated samples, nor did it after DCMU addition. The PAM probes the redox state of the quinone pool: the fact that light-induced stimulation of PSII by the PAM returns a null F_v in the dark implies that no photosynthetic electron transport was triggered, and so that operation of PSII was blocked. The present results ascertain that PSII is not operating in the dark period, invalidating the hypothesis that a transition to state II is the reason why cells show fully inefficient PSIIs. Whether cells do undergo state transition upon the dark onset or not, another phenomenon occurs that prevents electron transport from PSII during the dark period. Wilson et al. (2010) suggested that a reduction of the PQ pool by respiration operates in the dark. Our results point to a deeper effect on PSII regulation than the sole modification of the PQ redox status.

We believe that PSII is undergoing modifications in the dark, resulting in its inactivation or disconnection from the electron transport chain. Such behavior is very

different from what is observed in eukaryotes but also from other UCYN. For instance, PSII inhibition at night does not occur in the coastal strain *Cyanothece* BG43511 grown in obligate diazotrophy under LD regimes with 8 to 16 hours of light (Rabouille et al., 2013). In *Cyanothece*, transcriptional regulation operates to further optimize photosynthesis through the enhancement of either the non cyclic (PSII synthesis) or cyclic (PSI synthesis) electrons flow (Colon-Lopez and Sherman, 1998). It was also shown that cyanobacteria possess several psbA genes encoding for the D1 protein, some of which bearing mutations or alterations, rendering D1 inactive (Murray, 2012). In particular, Zhang and Sherman (2012) and Wegener et al (2015) demonstrated that in the genus *Cyanothece*, the alternate copies of psbA are transcribed into an inactive, D1 sentinel (sD1) under specific environmental conditions such as periods when nitrogen fixation is active. About half of *C. watsonii* genome shows a diel expression pattern (Shi et al., 2010), which includes genes coding for nitrogen fixation and photosynthesis. We believe that, because the loss of PSII efficiency is rather fast, the regulation in *C. watsonii* PSII complexes involves modifications or alterations at the protein level, leading to inactivation of the entire pool of PSII in cells. In their supplementary material, Shi and colleagues (2010) present a list of genes with diel expression patterns, showing that psbA1 (coding for D1) is expressed in the light and psbA4 (coding for sD1) is expressed in the dark. The present data thus support and confirm that sD1 encoded by psbA4 is indeed inactive. Further, *C. watsonii* cells share iron molecules between night-time and light-time processes, through the synthesis and degradation of metalloenzymes (Saito et al., 2011): not only nitrogenase is degraded daily but some iron-containing complexes of photosynthesis as well. The absence of photosynthetic capacity in the dark observed here suggests that the degradation of photosynthetic components described by Saito

and colleagues (2011) may follow the alteration of the photosynthetic apparatus structure described here.

220   **Cells prevent oxygen evolution at light transitions to allow for N_2 fixation in the light**

Nitrogen fixation can only occur as long as nitrogenase is present and active in cells. In UCYN, a de novo synthesis of nitrogenase accompanies the daily buildup of nitrogenase mRNA transcripts (Pennebaker et al., 2010; Shi et al., 2010), thereby

225   ensuring a temporal separation of nitrogen fixation from photosynthesis. But if disappearance of mRNA transcripts in the late dark period sets the moment when the nitrogenase enzyme pool is not synthesized anymore and can only decrease, cells seem not to exert any regulation on the activity of the enzyme, which keeps fixing nitrogen as long as it is uncorrupted. Nitrogen fixation is much more efficient in the

230   dark, yet fixation in the light can occur, whose extent is related to light periodicity and increases as the dark period gets shorter. *C watsonii* acquires in the light 0, 8 and 21 % of the total amount fixed over 24h, when the dark phase is reduced from 16h to 12 and 8 hours, respectively (Dron et al., 2013): under short dark periods, nitrogenase activity proceeds for several hours into the light.

235   Results from the literature illustrate the ability of *Crocosphaera* to sustain active nitrogen fixation in the light when the period theoretically devoted to this process is getting short. Our present analysis explains how *Crocosphaera* manages to do so, through a regulation on PSII. PSII activity falling down to zero before the end of the light phase in longer photoperiods (12L:12D and 16L:8D) will facilitate the onset of

240   nitrogen fixation. Conversely, energy shortage might be expected under short

photoperiods and PSII is then operational already in the late dark phase, to prepare for a possible photosynthetic activity as soon as light comes, and remains active beyond the end of the light period, to maximize energy acquisition.

Figure 5 compares the temporal dynamics of PSII efficiency (this study) to that of nitrogenase activity in the same cultures (Dron et al., 2012; Dron et al., 2013). In cyanobacteria, plastoquinone (PQ) is the first of the three electrons carriers shared between photosynthesis and respiration (Vermaas, 2001). Respiratory electron transfer mostly operates through the succinate dehydrogenase (Cooley et al., 2000), which reduces the PQ pool. PQ is thus a hub for all electron transport in cyanobacteria cells, and passes-on electrons to the following two, shared carriers: cytochrome b6f and plastocyanin. From the latter, electrons are either directed towards photosystem I (for photosynthesis) or to a terminal oxidase (for respiration). While the first route mostly predominates in the light, the second is the only one to proceed in the dark. In UCYN, significant electron flux in the dark originates from the high-energy requirement for nitrogen fixation. In the UCYN *Cyanothece* BG43511, the related changes in the redox state of the PQ pool were revealed through nighttime fluctuations in the PSII fluorescence kinetics, indicating that respiratory electron transport rate in the dark actually reflects the electrons demand for nitrogen fixation (Rabouille et al., 2013).

In the present study, we initially expected *C. watsonii* to show nighttime fluorescence dynamics similar to that reported for *Cyanothece*, as both operate nitrogen fixation in the dark. The observed, total absence of response in the dark is obviously very intriguing here and, to the best of our knowledge, hasn't been reported in any other photosynthetic organism so far. It was shown that respiration activity in *Cyanothece* sp. ATCC 51142 sharply increases before the onset of the dark when cultures are

grown under a 16L:8D regime and it was suggested that the purpose of such respiration peak was to create the microaerobic conditions required for nitrogenase to operate (Cerveny and Nedbal, 2009). Observation of net O_2 evolution and CO_2 consumption further comforted Cerveny and Nedbal (2009) to conclude that cells show a transition from a photosynthesis dominating, to a respiration dominating state, in the late light period. In *C. watsonii*, the observed modification of PSII follows nitrogenase dynamics more than the strict Light:Dark regime. Light shift is not the trigger and we believe instead that this regulation operates in tight synchrony with that of nitrogenase. Inactivation of PSII when nitrogenase is active will prevent any damage of the enzyme by evolved oxygen. From an ecological point of view, this phenomenon is part of the strategy that UCYN such as *C. watsonii* have evolved to further facilitate nitrogen fixation in a photosynthetic cell.

Experimental procedures

Experimental conditions

Experiments were performed on the non-axenic strain *C. watsonii* WH8501 (Waterbury and Rippka, 1989; Zehr et al., 2001). Three sets of continuous cultures, grown in duplicate, were brought to the equilibrium under different LD regimes. Description of the culture setup (Malara and Sciandra, 1991) and experimental conditions are already detailed in sister papers (Dron et al., 2012; Dron et al., 2013) and so only briefly recalled below. Culture vessels were double-walled, borosilicate glass photobioreactors with a working volume of 5 L. Temperature was constant at 27 degrees and controlled using a water bath. Irradiance was provided with fluorescent tubes (OSRAM, DULUX®L, 2G11, 55W/12–950, LUMILUX DE LUXE, daylight)

290   on each side of all cultures. Three different LD regimes were applied that reproduced

a bell shape representative of natural irradiance periodicity, with 16 hours light

(16L:8D), 12 hours light (12L:12D), and 8 hours light (8L:16D) (Fig. 2); all observed

the same maximum light intensity of 130 µmol photons m^{-2} s^{-1} at mid-day. Cultures

were permanently stirred (using a magnetic stirrer) and aerated with filtered air.

295   Transient cell dynamics in the cultures were monitored through daily cell counts,

using a Coulter Counter (Beckman). Establishment of the equilibrium phase was

marked by a stable, daily average of cell abundances in the cultures. Once at the

equilibrium, duplicate cultures were continuously monitored for several parameters

for four consecutive days, during both light and dark periods. Cell size distribution,

300   abundance, nitrogen fixation activity as well as carbon and nitrogen content have been

described in previous works (Dron et al., 2012; Dron et al., 2013). In the present

study, hourly records of fluorescence dynamics are analyzed and discussed in relation

to the activity of nitrogen fixation.

Photosystem II activity

305   Every hour in both cultures, the maximum energy conversion efficiency, or quantum

efficiency of PSII charge separation (F_v/F_m) was measured using a WATER/B – PAM

fluorometer (Walz, Effeltrich, Germany). Culture samples were either analyzed

immediately upon sampling, or first incubated in the dark for one to 10 minutes prior

to analysis, in order to determine whether the incubation time affects the fluorescence

310   response and triggers state transitions. The sample was excited by a weak blue light (1

µmol photons m^{-2} s^{-1}, 470 nm, frequency 0.6 kHz) to record minimum fluorescence

(F_0). Maximum fluorescence (F_m) was obtained during a saturating light pulse (0.6 s,

1700 µmol photons m^{-2} s^{-1}, 470 nm), allowing the quinone A (QA), quinone B (QB)

and part of plastoquinone (PQ) pools to be reduced. F_v/F_m was calculated according to

the following equation (Genty et al., 1989) after subtraction of the blank fluorescence,

measured on medium filtered through a GF/F glass-fibre filter:

$$F_v/F_m = (F_m - F_0)/F_m \tag{1}$$

The samples were exposed to nine irradiances (I) for 1 min each, covering a range

from zero up to 1190 µmol photons m^{-2} s^{-1}. Steady state fluorescence (F_t) and

maximum fluorescence (F_m') were measured. The effective quantum efficiency of

PSII at each irradiance was determined as follows (Genty et al., 1989).

$$F_v'/F_m' = (F_m' - F_t)/ F_m' \tag{2}$$

The relative electron transport rate (rETR, arbitrary unit) was calculated for each

irradiance. rETR is a measure of the rate of linear electron transport through

photosystem II.

$$rETR = F_v'/F_m' \cdot I \tag{3}$$

where I is the light intensity expressed as photosynthetically active radiations (µmol

photons m^{-2} s^{-1}) Following the approach proposed by Napoleon & Claquin (2012),

rETR *vs* irradiance data were fitted using the model proposed by Eilers and Peeters

(1988). The general form of this model reads:

$$rETR (I) = I / (a \cdot I^2 + b \cdot I + c) \tag{4}$$

However, in this expression, the parameter b shows unclear meaning from a

physiological point of view and, most importantly, calibration of the model is not

trivial. As proposed by Bernard and Rémond (2012), by changing the expression of

parameters within the same equation, it is possible to express α, the initial slope of the

PI curve, $rETR_{opt}$, the optimal rETR value observed in the PI curve, and I_{opt}, the

optimal irradiance (Fig. 1):

$$rETR\left(I\right) = rETR_{opt} \times \dfrac{I}{I + \dfrac{rETR_{opt}}{a} \times \left(\dfrac{I}{I_{opt}} - 1\right)^2} \qquad (5)$$

340 Time series of values for these three parameters were thus retrieved from the light-response curves. Comparison of I_{opt} and the ambient irradiance I informs on how close to optimal irradiance conditions cells are.

On the visualization and role of State Transitions

345 Dark incubation prior to chlorophyll fluorescence measurements is usually performed to progressively block the quenching effect by PSII and thereby reopen all reaction centers. In higher plants and eukaryotic algae, a ten-minute dark incubation or an exposure to far-red light (700-720nm) prior to the measurement is in practice enough to fully oxidize the quinone A (Q_A), the electron acceptor of PSII. The modulated,

350 low measuring light then applied with the PAM, which does not trigger any photochemistry, only leads to a very low fluorescence level (F_0). Upon application of a saturating flash, all reaction centers transiently close and Q_A is fully reduced, leading to a maximum fluorescence F_m. Under the intermediate irradiance levels applied when recording a PI curve, the transient fluorescence progressively rises,

355 indicating that more reaction centers are closing when ambient light levels increase. In cultures of *C. watsonii*, dark incubation led to PI records with a curved shape in the PSII yield at lower irradiances, instead of the usual, rather linear initial response. Such curvature denotes a lower PSII yield than what could be expected under favorable conditions, and also indicates that PSII yield builds up in time, as irradiance increases.

360 This behavior also shows on the F_m records (Fig. 4a); it is typical of state transition, actually triggered here by the dark exposure, in which phycobilisomes move along the

thylakoid membrane, away from PSII and attach to PSI (transition to state II). In green plants, state transitions are believed to play a photo protective role under excess illumination (Mullineaux and Emlyn-Jones, 2005). The primary purpose of state transitions in cyanobacteria is not photoprotective but rather allows cells to more efficiently deal with low light levels (Allen et al., 1989), as it modulates the excitation levels of photosystems I and II, through redistribution of energy between the two photosystems as described in Campbell and Oquist (1996) and Campbell et al. (1998).

PSII efficiency therefore decreases when cells transition to state II, as revealed by lower initial slopes (α) of the rETR light response curves recorded on dark-adapted samples. Even though state transitions are not best represented by ETR curves, the phenomenon was clearly visible in the ETR dynamics. Upon re-exposure to actinic light as the PI curve record proceeds, cells initiate a transition back towards state I; but the first PSII yields recorded at low irradiances do not reflect the actual PSII potential at these intensities as phycobilisomes are not yet re-attached to PSII. In this case, measured and modeled values of α underestimate the potential response of cells. From a technical point of view, this point illustrates how slight changes in PAM acquisition protocols can lead to very different estimations of photosynthetic efficiency at low lights. However, and importantly, this phenomenon did not alter the quantum yield at high light (F_v'/F_m'), from which we derived $rETR_{opt}$. Records demonstrated that recovery to state I was complete within the first minutes of actinic light exposure. As a corollary, two samples taken at the same time, one pre-incubated in the dark and the other not, always yielded similar $rETR_{opt}$.

Proper measures of F_v/F_m require DCMU (Campbell et al., 1998), which reveals possible state transitions. DCMU was added to the samples, after recording the PI curve and re-exposition to the dark. DCMU, which occupies the plastoquinone

binding site, actually prevents electrons from moving down the electron transport chain. As a result, photons captured by PSII are re-emitted as fluorescence, up to the maximum level F_m. The maximum level of fluorescence observed following DCMU

390 addition was much higher than the F_m value recorded during each PI curve, indicating that DCMU-treated cells transition much further into state I by attaching more phycobilisomes to PSII compared to non-treated cells (data not shown).

Acknowledgements

405

References

Allen, J.F., Mullineaux, C.W., Sanders, C.E., and Melis, A. (1989) State transitions, photosystem stoichiometry adjustment and non-photochemical quenching in

410   cyanobacterial cells acclimated to light absorbed by photosystem-I or photosystem-II. *Photosynth Res* **22**: 157-166.

Berman-Frank, I., Lundgren, P., Chen, Y.-B., Kupper, H., Kolber, Z., Bergman, B., and Falkowski, P. (2001) Segregation of nitrogen fixation and oxygenic photosynthesis in the marine cyanobacterium *Trichodesmium. Science* **294**: 1534-

415   1537.

Bernard O. and Rémond B. (2012) Validation of a simple model accounting for light and temperature effect on microalgal growth. *Biores Technol* **123**: 520–527.

Campbell, D. and Oquist, G. (1996) Predicting light acclimation in Cyanobacteria from nonphotochemical quenching of photosystem II fluorescence, which reflects

420   state transitions in these organisms. *Plant Physiol* **111**: 1293-1298.

Campbell, D., Hurry, V., Clarke, A.K., Gustafsson, P., and Oquist, G. (1998) Chlorophyll fluorescence analysis of cyanobacterial photosynthesis and acclimation. *Microbiol Mol Biol R* **62**: 667-683.

Cerveny, J., and Nedbal, L. (2009) Metabolic rhythms of the cyanobacterium

425   *Cyanothece* sp. ATCC 51142 correlate with modeled dynamics of circadian clock. *J Biol Rhythms* **24**: 295-303.

Colon-Lopez, M., Sherman, D., and Sherman, L. (1997) Transcriptional and translational regulation of nitrogenase in light- dark- and continuous-light-grown cultures of the unicellular cyanobacterium *Cyanothece* sp. strain ATCC 51142. *J*

430   *Bacteriol* **179**: 4319-4327.

Colon-Lopez, M.S., and Sherman, L.A. (1998) Transcriptional and translational regulation of photosystem I and II genes in light-dark- and continuous-light-grown cultures of the unicellular cyanobacterium *Cyanothece* sp. strain ATCC 51142. *J Bacteriol* **180**: 519-526.

435   Compaore, J., and Stal, L.J. (2010) Oxygen and the light-dark cycle of nitrogenase activity in two unicellular cyanobacteria. *Environ Microbiol* **12**: 54-62.

Cooley, J.W., Howitt, C.A., and Vermaas, W.F.J. (2000) Succinate:quinol oxidoreductases in the cyanobacterium *Synechocystis* sp. PCC 6803: presence and function in metabolism and electron transport. . *J Bacteriol* **182**: 714–722.

440   Dron, A., Rabouille, S., Claquin, P., Le Roy, B., Talec, A., and Sciandra, A. (2012) Light-Dark (12:12) cycle of carbon and nitrogen metabolism in *Crocosphaera watsonii* WH8501: relation to the cell cycle. *Environ Microbiol* **14**: 967-981.

Dron, A., Rabouille, S., Claquin, P., Talec, A., Raimbault, V., and Sciandra, A. (2013) Photoperiod length paces the temporal orchestration of cell cycle and carbon-

445   nitrogen metabolism in *Crocosphaera watsonii*. *Environ Microbiol* **15**: 3292–3304.

Eilers, P.H.C., and Peeters, J.C.H. (1988) A model for the relationship between light-intensity and the rate of photosynthesis in phytoplankton. *Ecol Model* **42**: 199-215.

Falcon, L.I., Cipriano, F., Chistoserdov, A.Y., and Carpenter, E.J. (2002) Diversity of diazotrophic unicellular cyanobacteria in the Tropical North Atlantic Ocean. *Appl*

450   *Environ Microbiol* **68**: 5760-5764.

Fay, P. (1992) Oxygen relations of nitrogen-fixation in cyanobacteria. *Microbiol Rev* **56**: 340-373.

Gallon, J.R. (1992) Reconciling the incompatible - N_2 Fixation and O_2. *New Phytol* **122**: 571-609.

455   Großkopf, T., and LaRoche, J. (2012) Direct and indirect costs of dinitrogen fixation in *Crocosphaera watsonii* WH8501 and possible implications for the nitrogen cycle. *Frontiers Microbiol*: doi: 10.3389/fmicb.2012.00236

Huang, T.C., Chow, T.J., and Hwang, I.S. (1988) The cyclic synthesis of the

nitrogenase of *Synechococcus* Rf-1 and its control at the transcription level. *FEMS*

460   *Microbiol Lett* **50**: 127-130.

Krause, G.H., and Weis, E. (1984) Chlorophyll fluorescence as a tool in plant

physiology .2. Interpretation of fluorescence signals. *Photosynth Res* **5**: 139-157.

Kromkamp, J.C., and Forster, R.M. (2003) The use of variable fluorescence

measurements in aquatic ecosystems: differences between multiple and single

465   turnover measuring protocols and suggested terminology. *Eur J Phycol* **38**: 103-

112.

Malara, G., and Sciandra, A. (1991) A multiparameter phytoplankton culture system

driven by microcomputer. *J Appl Phycol* **3**: 235-241.

Mitsui, A., Kumazawa, S., Takahashi, A., Ikemoto, H., Cao, S., and Arai, T. (1986)

470   Strategy by which nitrogen-fixing unicellular cyanobacteria grow

photoautotrophically. *Nature* **323**: 720-722.

Mohr, W., Intermaggio, M.P., and LaRoche, J. (2010) Diel rhythm of nitrogen and

carbon metabolism in the unicellular, diazotrophic cyanobacterium *Crocosphaera*

watsonii WH8501. *Environ Microbiol* **12**: 412-421.

475   Montoya, J.P., Holl, C.M., Zehr, J.P., Hansen, A., Villareal, T.A., and Capone, D.G.

(2004) High rates of N_2 fixation by unicellular diazotrophs in the oligotrophic

Pacific Ocean. *Nature* **430**: 1027-1032.

Mullineaux, C.W., and Allen, J.F. (1986) The state-2 transition in the cyanobacterium

Synechococcus 6301 can be driven by respiratory electron flow into the

480   plastoquinone pool. *FEBS Lett* **205**: 155-160.

Mullineaux, C.W., and Emlyn-Jones, D. (2005) State transitions: an example of

acclimation to low-light stress. *J Exp Bot* **56**: 389-393.

Murray, J.W. (2012) Sequence variation at the oxygen-evolving centre of photosystem II: a new class of 'rogue' cyanobacterial D1 proteins. *Photosynth Res* **110**: 177-184.

Napoleon, C., and Claquin, P. (2012) Multi-parametric relationships between PAM measurements and carbon incorporation, an in situ approach. *PLoS One* **7**.

Pennebaker, K., Mackey, K.R.M., Smith, R.M., Williams, S.B., and Zehr, J.P. (2010) Diel cycling of DNA staining and nifH gene regulation in the unicellular cyanobacterium *Crocosphaera watsonii* strain WH 8501 (Cyanophyta). *Environ Microbiol* **12**: 1001-1010.

Rabouille, S., Van de Waal, D.B., Matthijs, H.C.P., and Huisman, J. (2013) Nitrogen fixation and respiratory electron transport in the cyanobacterium *Cyanothece* under different light/dark cycles. *FEMS Microbiol Ecol* **87**: 630-638.

Saito, M.A., Bertrand, E.M., Dutkiewicz, S., Bulygin, V.V., Moran, D.M., Monteiro, F.M. et al. (2011) Iron conservation by reduction of metalloenzyme inventories in the marine diazotroph *Crocosphaera watsonii*. *Proc Natl Acad Sci U S A* **108**: 2184-2189.

Shi, T., Ilikchyan, I., Rabouille, S., and Zehr, J.P. (2010) Genome-wide analysis of diel gene expression in the unicellular N-2-fixing cyanobacterium *Crocosphaera watsonii* WH 8501. *Isme J* **4**: 621-632.

Staal, M., Rabouille, S., and Stal, L.J. (2007) On the role of oxygen for nitrogen fixation in the marine cyanobacterium *Trichodesmium* sp. *Environ Microbiol* **9**: 727-736.

Toepel, J., Welsh, E., Summerfield, T.C., Pakrasi, H.B., and Sherman, L.A. (2008) Differential transcriptional analysis of the cyanobacterium *Cyanothece* sp strain

ATCC 51142 during light-dark and continuous-light growth. *J Bacteriol* **190**: 3904-3913.

Vermaas, W.F.J. (2001) Photosynthesis and respiration in cyanobacteria. In: Encyclopedia of Life Sciences. John Wiley & Sons (eds), New York.

Waterbury, J.B., and Rippka, R. (1989) The order *Chroococcales*. In Bergey's Manual of Systematic Bacteriology. Krieg, N. R., and Holt, J. B. (eds.), pp.: 1728-1746.

Waterbury, J.B., Watson, S.W., and Valois, F.W. (1988) Temporal separation of photosynthesis and dinitrogen fixation in the marine unicellular cyanobacterium *Erythrosphaera marina*. *EOS* **69** 1089.

Wegener, K.M., Nagarajan, A., and Pakrasi, H.B. (2015) An atypical *psbA* gene encodes a sentinel D1 protein to form a physiologically relevant Inactive photosystem II complex in Cyanobacteria. *J Biol Chem* **290**: 3764-3774.

Wilson, S.T., Tozzi, S., Foster, R.A., Ilikchyan, I., Kolber, Z.S., Zehr, J.P., and Karl, D.M. (2010) Hydrogen cycling by the unicellular marine diazotroph *Crocosphaera watsonii* Strain WH8501. *Appl Environ Microbiol* **76**: 6797-6803.

Zarmi, Y., Bel, G., Aflalo, C. (2013) Theoretical analysis of culture growth in flat-plate bioreactors: the essential role of timescales. 2nd ed. in: *Handbook of Microalgal Culture*, (Eds.) A. Richmond, Q. Hu, Wiley-Blackwell, pp. 205-224.

Zehr, J.P. (2011) Nitrogen fixation by marine cyanobacteria. *Trends Microbiol* **19**: 162-173.

Zehr, J.P., Waterbury, J.B., Turner, P.J., Montoya, J.P., Omoregie, E., Steward, G.F. et al. (2001) Unicellular cyanobacteria fix N_2 in the subtropical North Pacific Ocean. *Nature* **412**: 635-638.

530   Zhang, X.H., and Sherman, L.A. (2012) Alternate copies of D1 are used by

cyanobacteria under different environmental conditions. *Photosynth Res* **114**: 133-

135.

Titles and legends to figures

535

Figure 1

Typical light response curve of the relative electron transport rate (rETR) recorded in the light phase on cultures of *C. watsonii*. Measurements (closed diamonds) are plotted as a function of the irradiance level applied at each step when recording the

540 light response curve. The according model simulation (black line) is represented, from which is deduced the optimal rate ($rETR_{opt}$) and optimal irradiance (I_{opt}).

Figure 2

545 Variable fluorescence dynamics recorded for four consecutive days in the duplicate cultures, under the 16L:8D (1a), 12L:12D (1b) and 8L:16D (1c) regimes. The maximum, relative electron transport rate ($rETR_{opt}$) for culture 1 (open circle) and culture 2 (cross) as well as the bell-shaped irradiance dynamics (PAR, grey curve) are plotted in time. Dark periods are identified by dark grey areas. The time interval

550 between ticks on the x axis is 8 hours.

Figure 3

Diel dynamics of the fitted parameters $rETR_{opt}$ (a,b,c), α (d,e,f) and I_{opt} (g,h,i), obtained from the PI curves recorded in the duplicate cultures under the 16L:8D (a, d,

555 g), 12L:12D (b, e, h) and 8L:16D (c, f, i) regimes. In the latter regime, distinction was made between culture 1 (open circles, black regression line) and culture 2 (cross,

dashed regression line). The bell-shaped irradiance dynamics (grey curve) is recalled in graphs a, b and c. The time interval between ticks on the x axis is 4 hours.

560 **Figure 4**

Maximum (F_m, closed circles) and transient (F_t, crosses and triangles) fluorescence levels measured when recording light response curves during either the light phase (a), the first hour of light (b) or the dark phase (c). In (a), the grey and black color code is used to distinguish the {F_m, F_t} couple from a same record: in the light phase,

565 $F_m > F_t$. In contrast, at the dark-to-light transition (b) and in the dark (c), the different records all show $F_m = F_t$, illustrating why F_v is null.

Figure 5

Compared, average dynamics of $rETR_{opt}$ (grey curve) and nitrogen fixation (grey

570 area), for cultures exposed to a 16L:8D (a), 12L:12D (b) and 8L:16D (c) light regime. Graphs show a 24h period, the dark phase is symbolized by horizontal dark bars at the top of each graph. The x axis indicates hours into the light (L) or dark (D) period, with a two-hour time interval between ticks. Time starts with the first hour of dark. Records of nitrogen fixation activity were normalized and averaged (a: n= 7; b: n=2;

575 c: n=6). In (a) and (b) the $rETR_{opt}$ curve is a smoothed interpolation using all pooled data (n=4 records for each culture replicate). In (c), $rETR_{opt}$ dynamics is expressed using the regression curves from figure 3c and distinguishes the two replicates, due to the observed difference in amplitude between them.
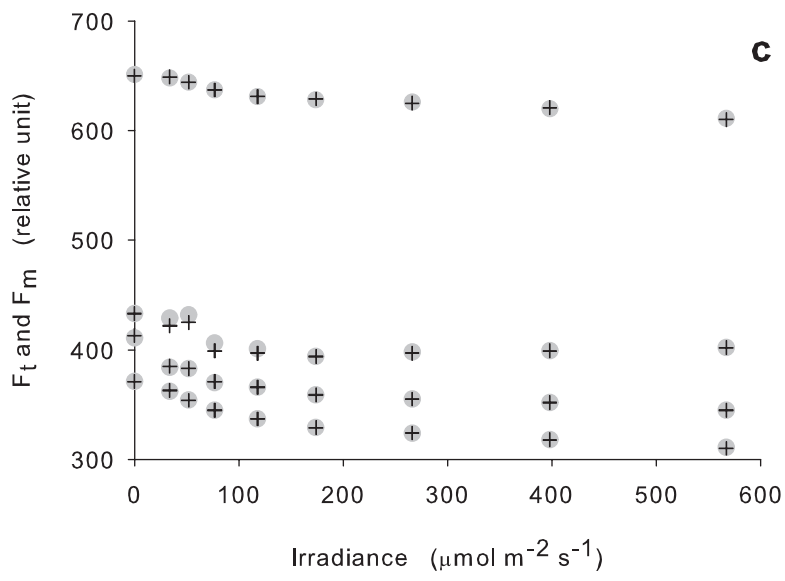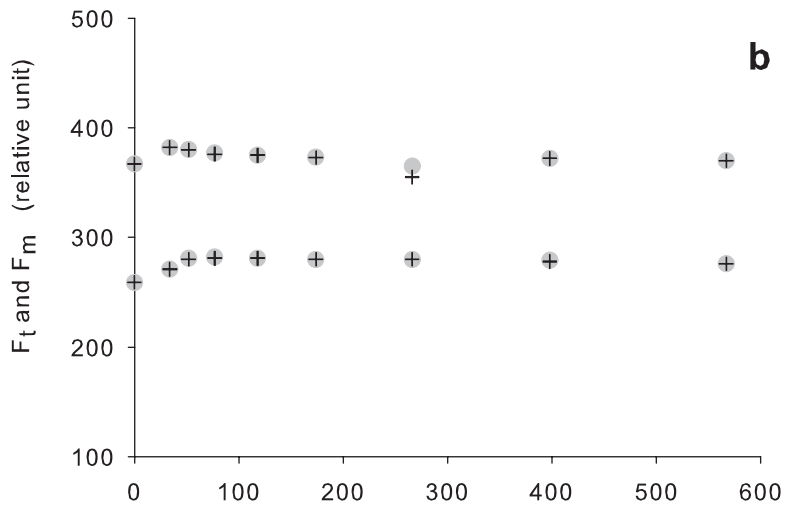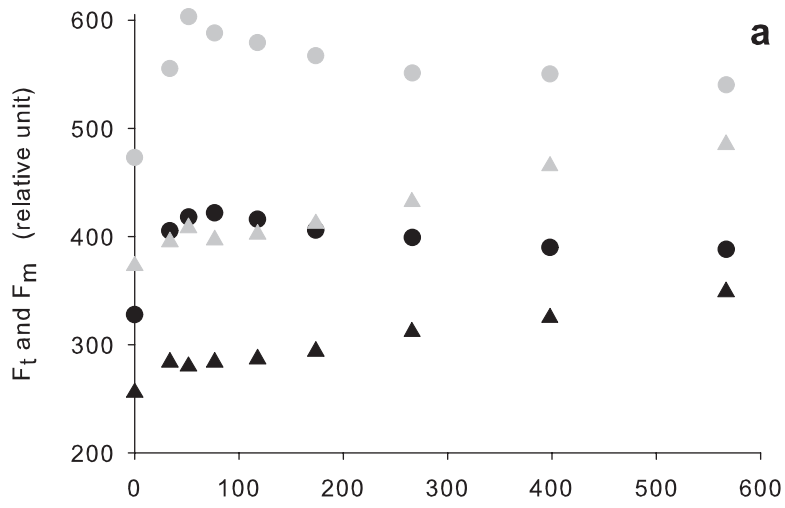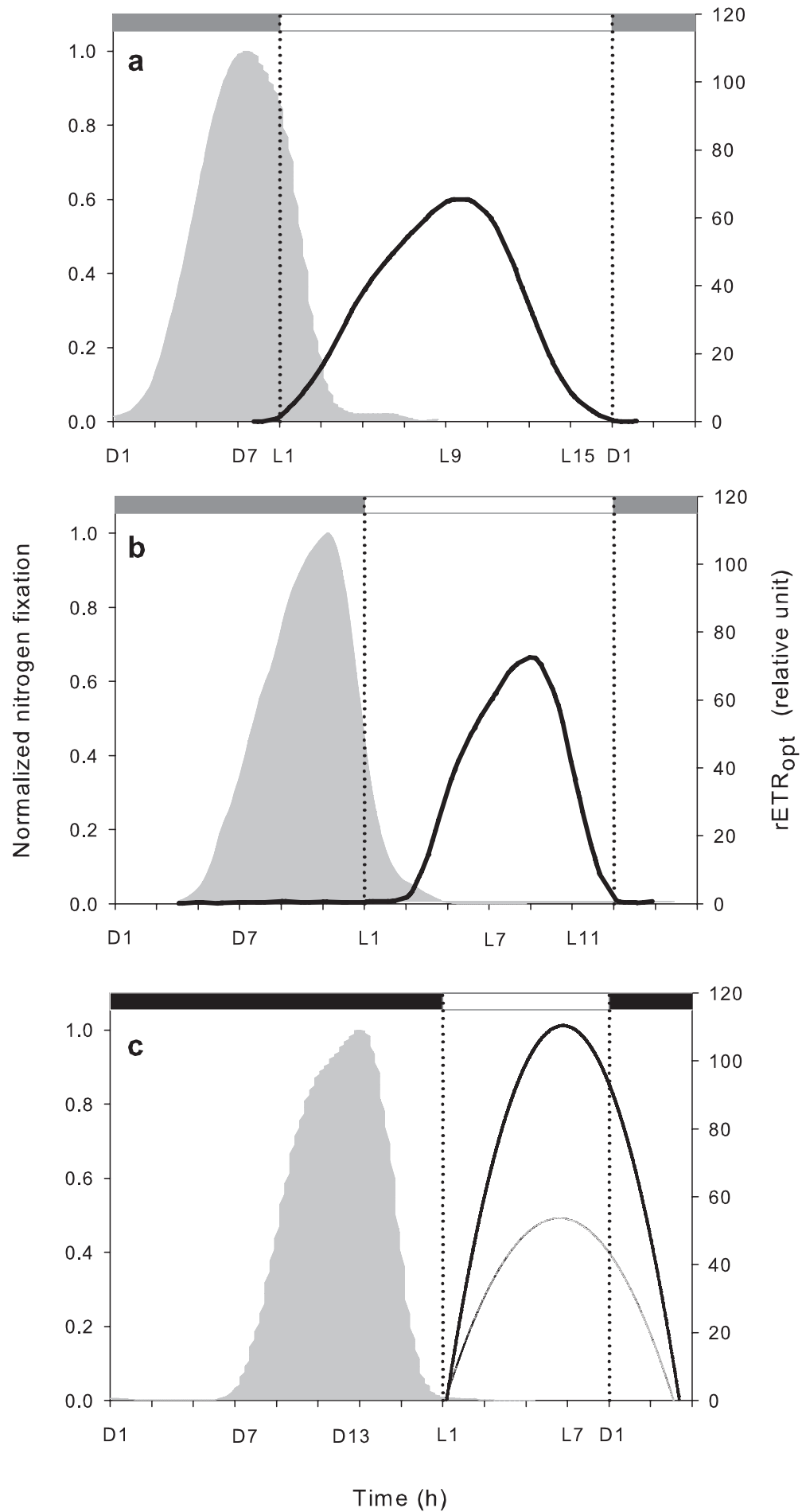
580

Rabouille & Claquin, Figure 1
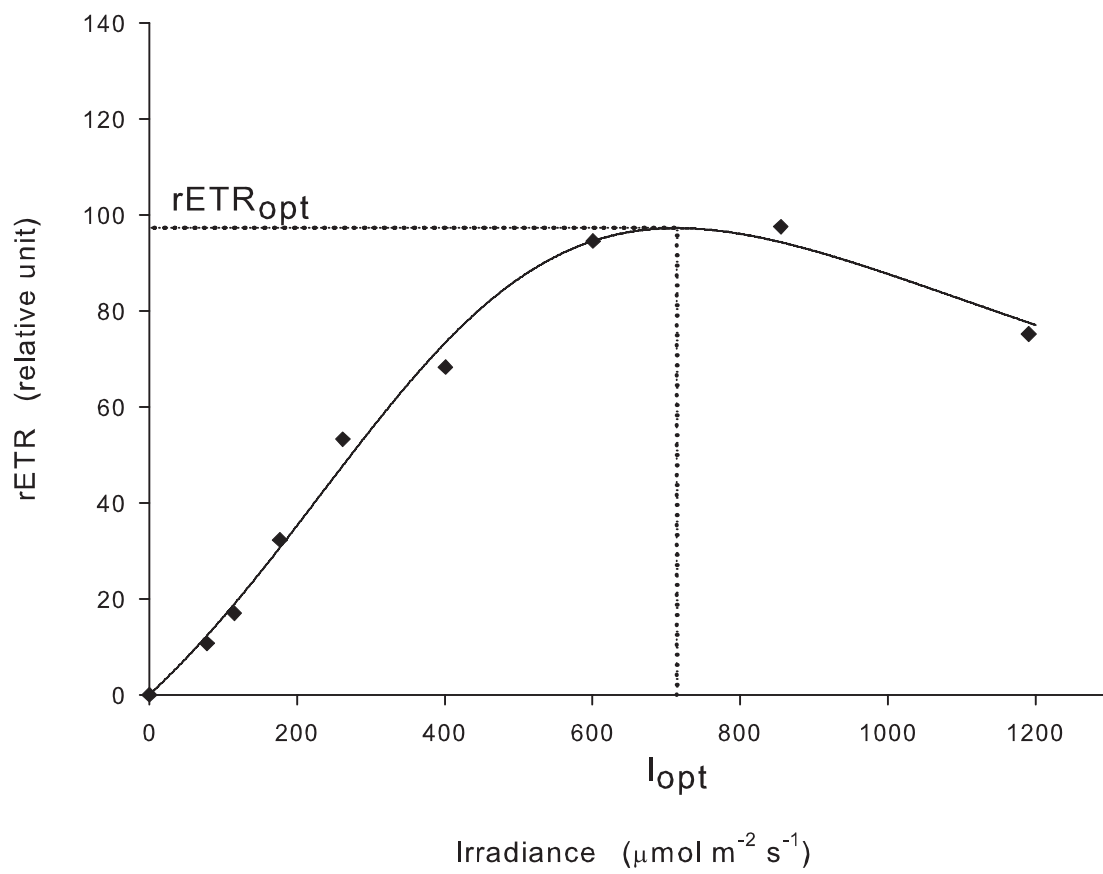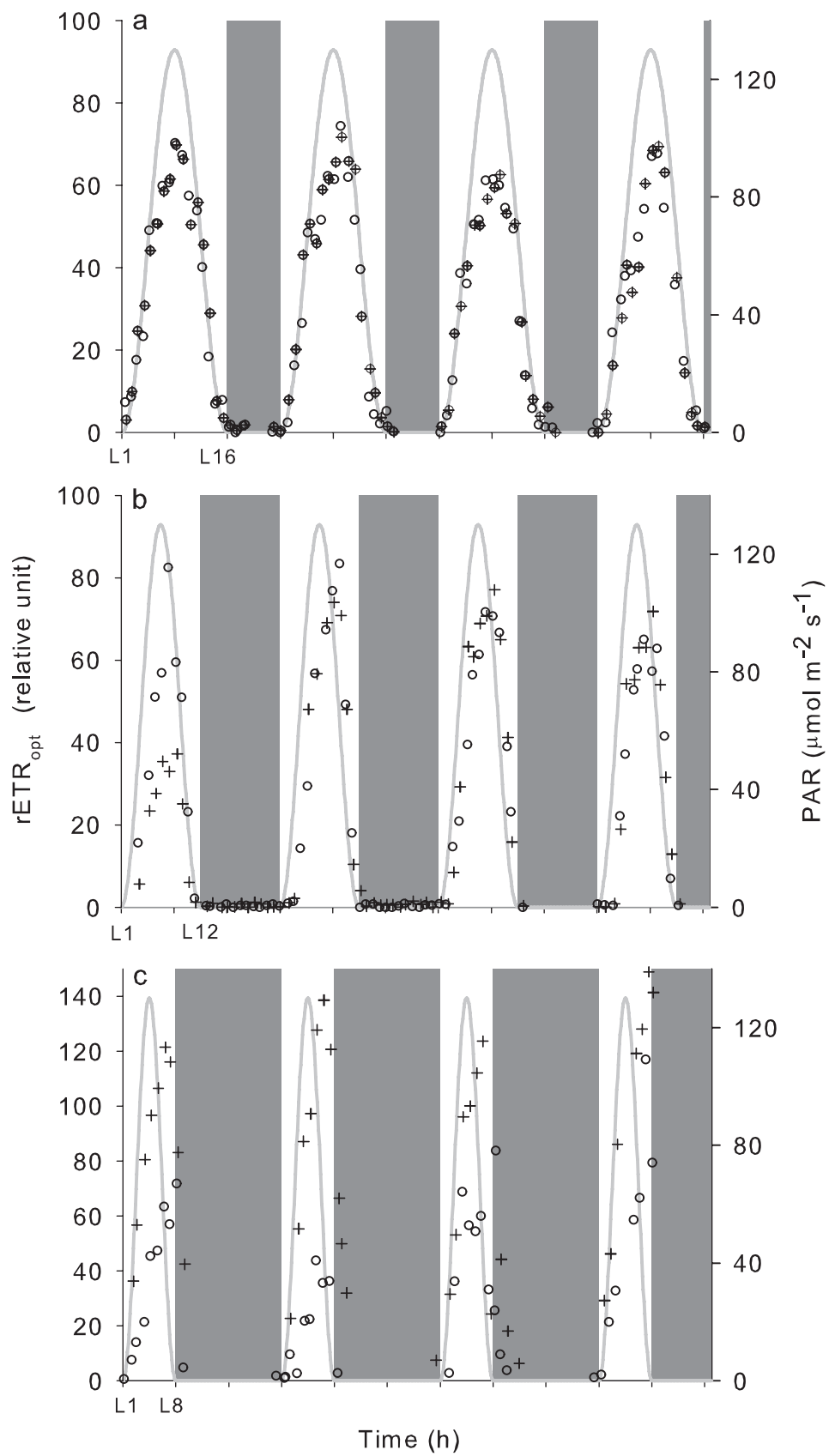
Rabouille & Claquin, Figure 2
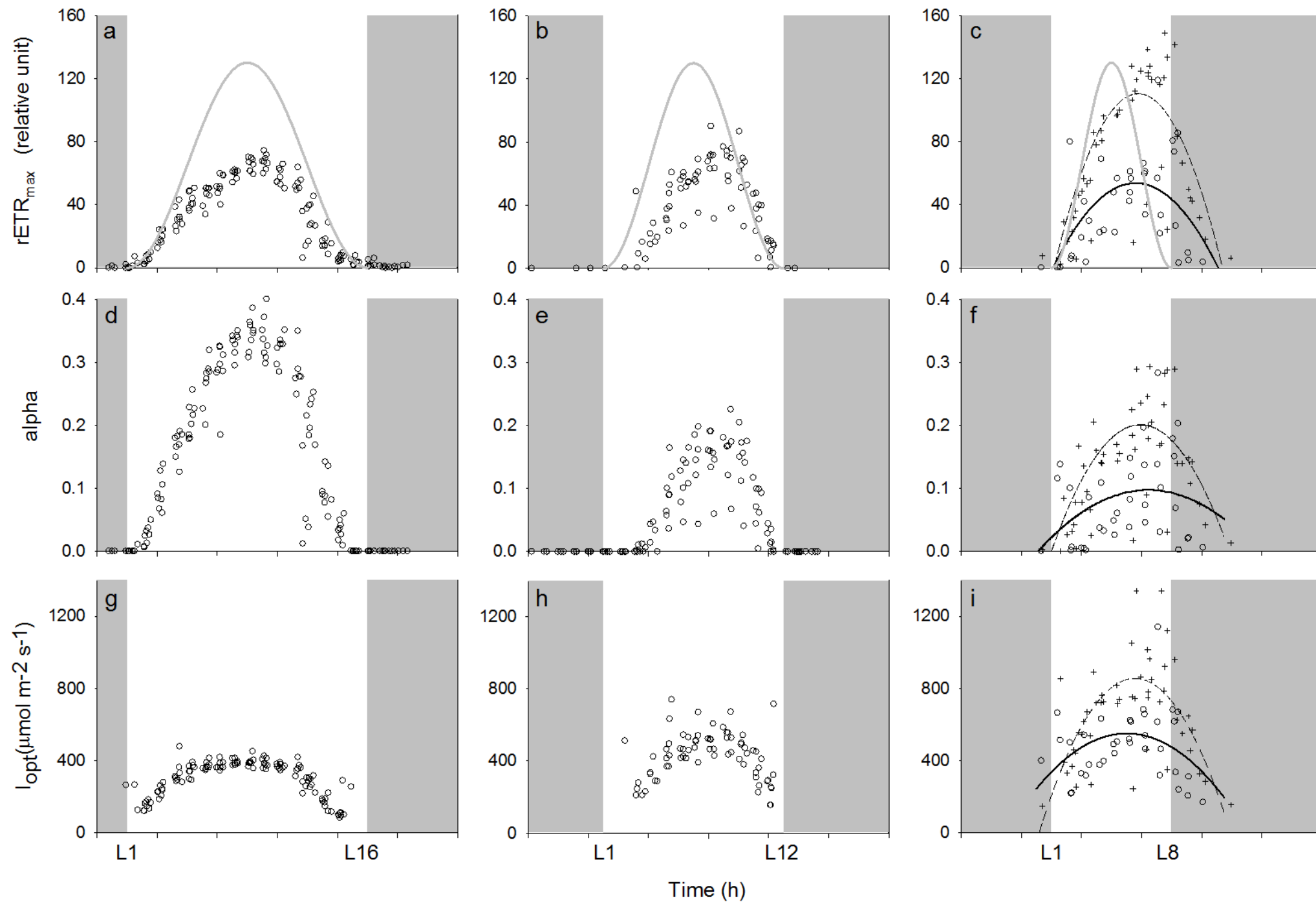
Rabouille & Claquin, Figure 3

Rabouille & Claquin, Figure 4

Rabouille & Claquin, Figure 5